

Characterization of covalent Ene adduct intermediates in “hydride equivalent” transfers in a dihydropyridine model for NADH reduction reactions

R. Daniel Libby*, Ryan A. Mehl¹

Moravian College, Chemistry Department, Bethlehem, PA 18018, United States

ARTICLE INFO

Article history:

Received 8 August 2011

Available online 20 October 2011

Keywords:

NADH model
Dihydropyridine
Hydride transfer
Ene reaction
Retro-Ene reaction
Ene-adduct
Mechanism
Transition state structure

ABSTRACT

A study of the reactions of an NADH model, 1,4-di(trimethylsilyl)-1,4-dihydropyridine, **7**, with a series of α,β -unsaturated cyano and carbonyl compounds has produced the first direct evidence for an obligatory covalent adduct between a dihydropyridine and substrate in a reduction reaction. The reactions were monitored by NMR spectroscopy. In all reactions studied, the covalent adduct was the first new species detected and its decomposition to form products could be observed. Concentrations of adducts were sufficiently high at steady-state that their structures could be determined directly from NMR spectra of the reaction mixtures; adduct structures are those expected from an Ene reaction between **7** and the substrate. This first reaction step results in transfer of the C₄ hydrogen nucleus of **7** to the substrate and formation of a covalent bond between C₂ of the dihydropyridine ring and the substrate α -atom. Discovery of these Ene-adduct intermediates completes the spectrum of mechanisms observed in NADH model reactions to span those with free radical intermediates, no detectable intermediates and now covalent intermediates. The geometry of the transition state for formation of the Ene adduct is compared with those of theoretical transition state models and crystal structures of enzyme–substrate/inhibitor complexes to suggest a relative orientation for the dihydropyridine ring and the substrate in an initial cyclic transition state that is flexible enough to accommodate all observed mechanistic outcomes.

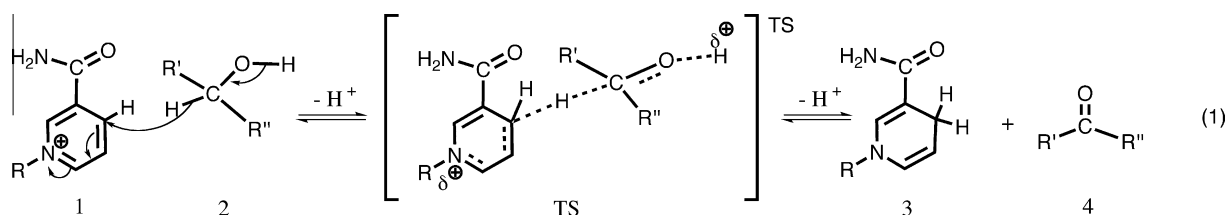
© 2011 Elsevier Inc. All rights reserved.

1. Introduction

Since Westheimer et al. [1] demonstrated that there is a direct hydrogen transfer from ethanol to NAD⁺ in the alcohol dehydrogenase catalyzed reaction, much work has been focused on the chemical mechanism of this transfer [2]. Both radical and ionic mechanisms have been proposed but to date no direct conclusive evidence for any covalent intermediate species has been presented for any enzymatic or model nicotinamide hydride transfer

reaction. Thus, the currently prevailing enzymatic mechanistic model is a one-step hydride transfer process, often referred to as a “hydride equivalent transfer”, which is generally written as in Eq. (1) with a transition state (TS) that has C4 of the nicotinamide ring (**1**), the H nucleus being transferred, and the carbon and oxygen atoms of the substrate (**2**) collinear.

In 1971 Hamilton proposed an ionic mechanism in which the hydrogen transfer from substrate to NAD⁺ is accomplished through an electrocyclic reaction [3]. Hamilton’s mechanism (Eq. (2))



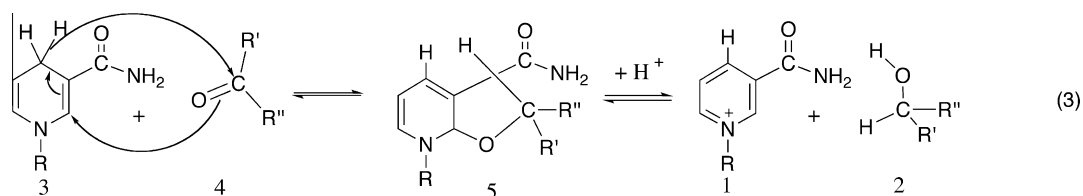
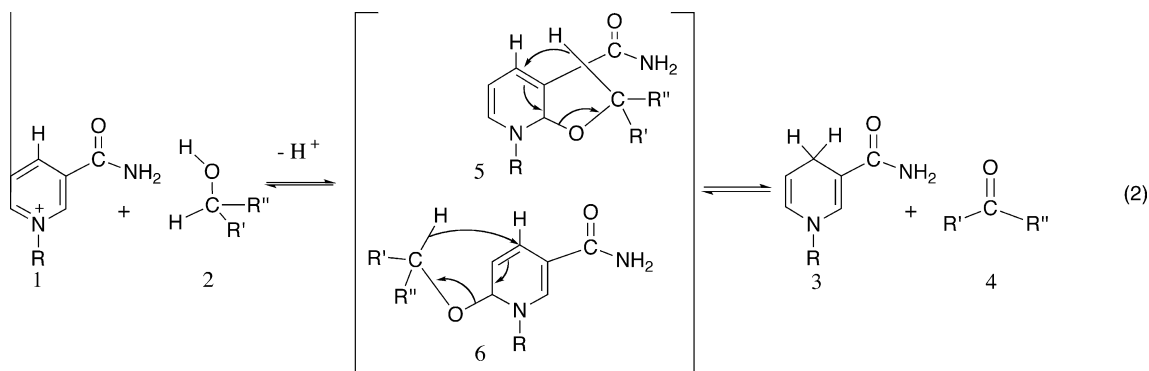
* Corresponding author. Fax: +1 610 625 7918.

E-mail address: rllibby@chem.moravian.edu (R.D. Libby).

¹ Present address: Department of Biochemistry & Biophysics, 2011 Agricultural Life Sciences Building, Oregon State University, Corvallis, OR 97331-7305, United States.

requires an intermediate, **5** or **6**, with a covalent bond between the oxygen atom of the substrate (**2**) and either C2 or C6 of NAD⁺ (**1**).

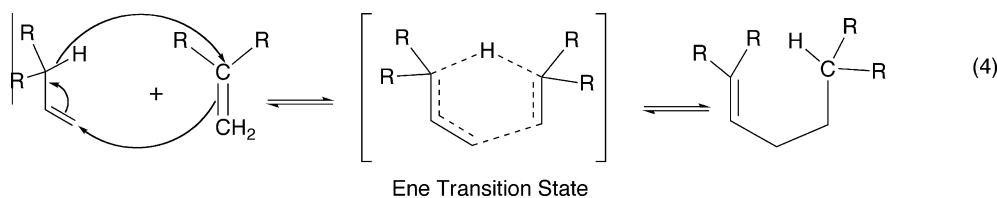
The first step of Hamilton’s mechanism is a nucleophilic addition of **2** to the iminium function of the NAD⁺ (**1**). The second step



is a cyclic intramolecular hydrogen transfer known as a Retro-Ene reaction, a well-documented pathway for decomposition of allyl ethers and thioethers [4].

When the reaction of Eq. (2) is viewed in the reverse direction (Eq. (3)), the first step is seen to be an electrocyclic Ene reaction, a type of reaction first characterized by Alder et al. in 1943 [5]. We will refer to the mechanism proposed by Hamilton as the Ene mechanism for hydride transfer in nicotinamide reactions. Ene reactions involve transition states with aromatic character,

completing the spectrum of mechanisms observed in NADH model reactions from those with single electron transfers, to apparently concerted hydride transfers (no detectable intermediates) [2] and now to Ene reactions (covalent intermediate Ene-adducts characterized). The Ene mechanism also suggests a relative orientation for the dihydropyridine ring and the substrate in an initial cyclic transition state that is flexible enough to accommodate all of the observed mechanisms.



which contributes to lowering their energies (Eq. (4)) [4].

Because of a lack of evidence for covalent intermediates in NADH reactions, the Ene mechanism for hydride transfer has not received much consideration in the literature. We now report the direct NMR observation of covalent intermediates in the reduction of a series of α,β -unsaturated cyano and carbonyl compounds (**8a–e**) by 1,4-di(trimethylsilyl)-1,4-dihydropyridine, **7** (Fig. 1). Although our model is quite different from NADH, our observations support the fundamental possibility of involvement of the Ene mechanism for hydride transfer in dihydropyridine reactions

2. Experimental

2.1. General

Acrylonitrile (2-propenenitrile, **8a**) (Sigma–Aldrich) was distilled while protected from moisture with CaCl_2 drying tubes and was stored under argon until used, tetrahydrofuran (Sigma–Aldrich) was purified by drying with LiAlH_4 and distillation under a positive argon pressure with protection by CaCl_2 drying tubes [6], pyridine (Sigma–Aldrich) was distilled and stored under argon until used,

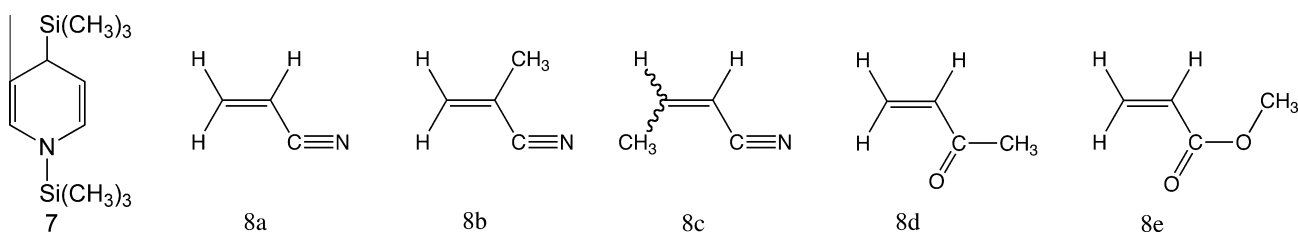


Fig. 1. 1,4-ditrimethylsilyl-1,4-dihydropyridine, **7** and α,β -unsaturated cyano and carbonyl electron accepting reagents: acrylonitrile, **8a**; methacrylonitrile, **8b**; (*E,Z*) crotonitrile, **8c**; methyl vinyl ketone, **8d**; methyl acrylate, **8e**.

98% chlorotrimethylsilane (Sigma–Aldrich) was distilled and stored under argon until used. 1,4-Di(trimethylsilyl)-1,4-dihydropyridine (**7**) was synthesized according to the method of Sulzbach and characterized by ^1H NMR [7]. (5.66 δ doublet $J = 7.4$ Hz, 4.25 δ doublet of doublets $J = 4.3$ and 7.6 Hz, 2.11 δ triplet $J = 4.3$ Hz, 0.09 δ singlet, 0.00 δ singlet) The air sensitive product was purified by vacuum distillation and stored under argon. It had minor impurities of 4-trimethylsilylpyridine, **12** (^1H NMR: 7.40 δ doublet of doublets, 8.45 δ doublet of doublets, 0.24 δ singlet) and a hydrocarbon possibly from pump oil. Neither impurity caused any problem with the reactions or analyses. Other reagents were from Sigma–Aldrich and used as supplied.

2.2. Reactions of 1,4-di(trimethylsilyl)-1,4-dihydropyridine (**7**) with α,β -unsaturated compounds

All reactions were carried out in 5 mm NMR tubes under an argon atmosphere. NMR spectra were obtained at 200 MHz in a Varian XL200 Spectrometer. Ultraviolet–Visible absorption spectra were obtained in a Perkin–Elmer Lambda 6 spectrometer using 1 cm quartz cells.

2.3. Reactions of acrylonitrile (propenenitrile) (**8a**) with **7** in chloroform-*d*

The reaction mixture consisted of 200 μL (0.6 μmol) of **7**, 60 μL (0.9 μmol) of acrylonitrile and 500 μL chloroform-*d*. The reaction mixture was maintained at room temperature and analyzed by ^1H NMR periodically for 71 h.

2.4. Reactions of acrylonitrile (propenenitrile) (**8a**) with **7** in acetone-*d*₆/H₂O

The reaction mixture consisted of 200 μL (0.6 μmol) of **7**, 40 μL (0.6 μmol) of acrylonitrile, 500 μL acetone-*d*₆ and 12 μL H₂O (0.7 μmol). The reaction mixture was maintained at 50 °C for 210 h and monitored periodically by ^1H NMR.

2.5. Reactions of methacrylonitrile (2-methyl-propenenitrile) (**8b**) with **7** in chloroform-*d*

The reaction mixture, consisting of 200 μL (0.6 μmol) of **7**, 60 μL (0.9 μmol) of methacrylonitrile 500 μL chloroform-*d*, was maintained at room temperature for 124 h. The mixture was then heated at 48 °C for an additional 94 h. During the course of the reaction the mixture was monitored periodically by ^1H NMR.

2.6. Reactions of (*E,Z*) crotononitrile ((*E,Z*) 2-butenenitrile) (**8c**) with **7** in chloroform-*d*

The reaction mixture, consisting of 200 μL (0.6 μmol) of **7**, 60 μL (0.9 μmol) of (*E,Z*) crotononitrile 500 μL chloroform-*d*, was maintained at room temperature for 120 h. The mixture was then heated at 48 °C for an additional 70 h; total reaction time was 190 h. During the course of the reactions the mixture was monitored periodically by ^1H NMR.

2.7. UV analysis of **9a**

Compound **9a** was produced by reaction of acrylonitrile (**8a**) with **7** in THF. The reaction mixture consisted of 5.0 mL (15 μmol) of **7**, 5.0 mL (83 μmol) of acrylonitrile and was magnetically stirred at room temperature under an argon atmosphere. The reaction progress was monitored periodically by removal of 2.0 μL aliquots of reaction mixture and diluting them into 3 mL of THF. The spectra were scanned from 190 to 440 nm. The initial spectrum of **7** before

addition of **8a** showed a λ_{max} at 265 nm. Acrylonitrile showed no significant absorption in the region 190–440 nm. Over time the 265 nm absorption band decreased and a band at higher wavelength appeared. After 24 h of reaction when there was no further change in the absorption spectrum, it exhibited a λ_{max} at 326 nm.

2.8. Reactions of methyl vinyl ketone(3-buten-2-one) (**8d**) with **7** in chloroform-*d*

The reaction mixture consisted of 200 μL (0.6 μmol) of **7**, 60 μL (0.7 μmol) of methyl vinyl ketone and 500 μL chloroform-*d*. The mixture was maintained at room temperature for 198 h and monitored periodically by ^1H NMR.

2.9. Reactions of methyl vinyl ketone(3-buten-2-one) (**8d**) with **7** in acetone-*d*₆

The reaction mixture, consisting of 200 μL (0.6 μmol) of **7**, 50 μL (0.6 μmol) of methyl vinyl ketone and 500 μL acetone-*d*₆, was maintained at room temperature for 139 h and monitored periodically by ^1H NMR.

2.10. Reactions of methyl vinyl ketone(3-buten-2-one) (**8d**) with **7** in acetone-*d*₆/H₂O

The reaction mixture, consisting of 200 μL (0.6 μmol) of **7**, 50 μL (0.6 μmol) of methyl vinyl ketone, 500 μL acetone-*d*₆ and 12 μL H₂O (0.7 μmol), was maintained at room temperature for 144 h and monitored periodically by ^1H NMR.

2.11. Reactions of methyl acrylate(methyl propenoate) (**8e**) with **7** in acetone-*d*₆/H₂O

The reaction mixture, consisting of 200 μL (0.6 μmol) of **7**, 54 μL (0.6 μmol) of methyl acrylate, 500 μL acetone-*d*₆ and 22 μL H₂O (1.2 μmol), was maintained at room temperature for 10 min and then heated at 50 °C for 196 h. During the course of the reaction the mixture was monitored periodically by ^1H NMR.

3. Results

All of the reactions of **7** with acceptor substrates, **8a–8e** (Fig. 1), were monitored by ^1H NMR allowing direct observation of intermediates as they formed in the reaction mixture. For each reaction the initial ^1H NMR spectrum for the reaction mixture consisted of a combination of the spectra of **7** and **8** and a small amount of irremovable impurities, 4-trimethylsilylpyridine, **12**, and an inert hydrocarbon. All reaction NMR spectra not included as stacked time point sets and all NMR spectral characteristics of reactants, products and reaction intermediates are provided in Figs. A1–A6 and Tables A1–A7.

3.1. Reactions of α,β unsaturated cyano substrates

3.1.1. In chloroform-*d* solution

Reaction of **7** with acrylonitrile, **8a**, in chloroform-*d* yields diastereomeric Ene-adducts **9a**_(1&2) (Fig. 2). As the reaction proceeds the signals from **7** to **8a** decrease, new series of signals for **9a**_(1&2) continually increase and no other new signals could be observed. Either the formation of **9a**_(1&2) from **7** to **8a** is a concerted process or any intermediates formed produced concentrations too low to be detectable by NMR.

The new signals consist of two sets that differ in intensity because **9a** consists of two diastereomeric pairs (**9a**₁ and **9a**₂) due to creation of two adjacent stereogenic centers in its formation

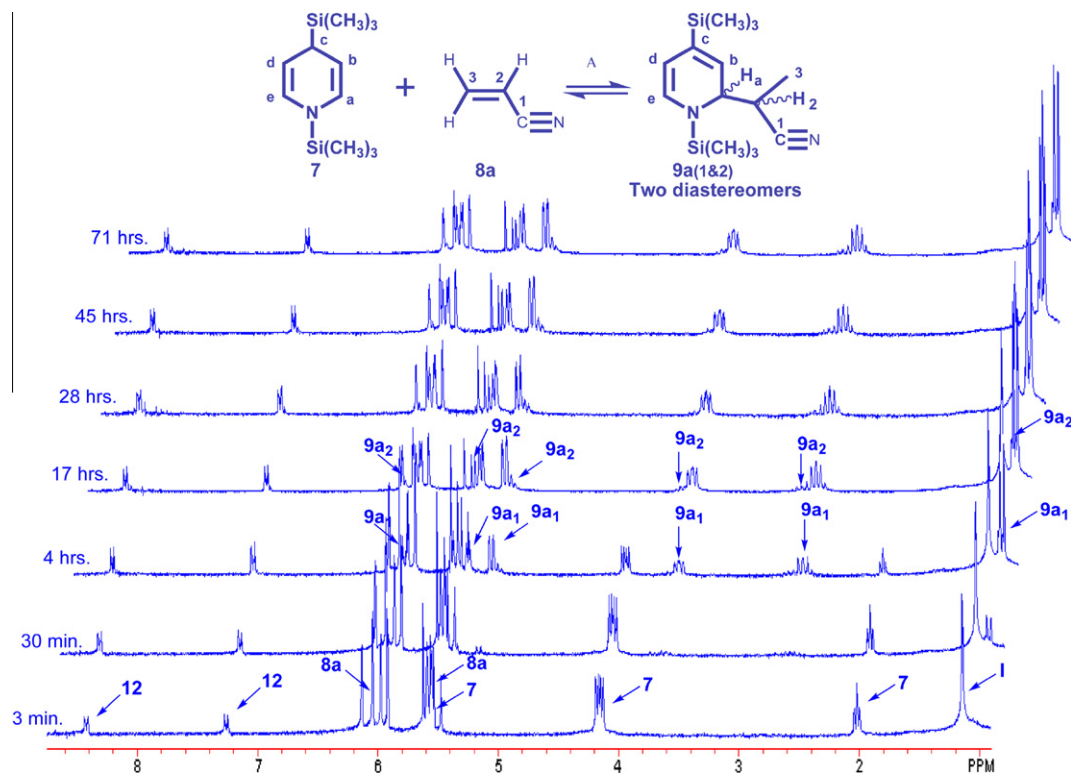


Fig. 2. Reaction of 1,4-di(trimethylsilyl)-1,4-dihydropyridine, **7**, with acrylonitrile, **8a**, in chloroform-*d*. Spectra at different time points: starting materials **7** and **8a** and irremovable impurities **12** and **I** from **7** are labeled in the first time point. Products **9a₁** and **9a₂** are labeled at times when they were first characterizable. Chemical shifts: **7**: H(a&e) 5.66 δ d, H(b&d) 4.25 δ dd, Hc 2.11 δ t; **8a**: H₂ 5.63 δ dd, H_{3_{cis}} 6.04 δ dd, H_{3_{trans}} 6.19 δ dd, I: 1.24 δ s; **9a₁**: Ha 3.81 δ dd, Hb 5.56 δ d, Hd 5.37 δ d, He 6.09 δ d, H2 2.78 δ dq, H3 1.12 δ d; **9a₂**: Ha 3.86 δ dd, Hb ~5.5 δ d, Hd 5.29 δ d, He 6.20 δ d, H2 2.90 δ dq, H3 1.14 δ d; **12**: H(a&e) 8.45 δ dd, H(b&d) 7.40 δ dd. (See Tables A1–A3 for coupling constants.)

(Fig. 2, positions a and 2). Product **9a₁** was first barely detected after 30 min of reaction and was characterizable after 4 h. The less intense set of peaks associated with **9a₂** was detectable after 4 h and was characterizable after 17 h. The 3.86 δ and 2.90 δ signals of **9a₂** partially overlap with the **9a₁** signals at 3.81 δ and 2.78 δ , and the **9a₂** signal in the 5.5 δ region is likely obscured by the 5.56 δ signal of **9a₁**. Similar newly formed chiral centers were also detected in reaction products from the reactions of **7** with **8b** and **8c** (Figs. A1 and A2 and Table A3; see **9b** and **9c**).

The **9a** diastereomers were formed in a ratio of approximately **9a₁**:**9a₂** = 5:1 based on the relative integrations of the 1.14 and 1.12 δ signals. After 17 h, the spectrum of **7** was no longer detectable and there were no further changes in the reaction spectrum for the additional 54 h that the reaction was monitored. Throughout the course of the reaction, the ¹H NMR signals from **12** did not change in intensity. Compound **12** is a decomposition product of both **7** and **9a** (See Section 3.1.2), so the lack of change in its signals is a further indication that **7** reacts only with **8a** and that **9a** is stable under the reaction conditions. Reactions of **7** with methacrylonitrile (2-methylpropenenitrile), **8b**, and crotonitrile (a mixture of *E*- and *Z*-2-butenitrile), **8c**, produced results very similar to that of **7** with **8a** but differing in the rate of the reactions (Appendix 1.1 and 1.2). The relative rate of appearance of the Ene products were **9a** > **9b** > **9c** judged from the relative times of appearance of **9** intermediates in Fig. 2, A1, and A2 and the relative integrations of the terminal methyl groups of **9a**, **9b** and **9c**. (Fig. A3) All cyano products studied, **9a–c**, are stable in chloroform-*d* solution. Similar results were obtained when reaction were run in acetone-*d*₆.

3.1.2. In acetone-*d*₆/H₂O solution

When water is present in the reaction of **7** with **8a** in acetone-*d*₆ (Fig. 3), the first detectable intermediate signals, **9a₁** and **9a₂**, were

first observed after 15 min of reaction and were intense enough to be characterized after 2 h. These first new intermediate spectra match those from products from the slower reaction of **7** and **8a** in chloroform-*d* or acetone-*d*₆ in the absence of water (See Section 3.1.1 and Tables A1–A5). After 4 h reaction in acetone-*d*₆/H₂O a second new set of signals, **10a**, was detected and characterizable after 40 h (Fig. 3 and Table A4). Intermediate **10a** is formed by the loss of the trimethylsilyl group from the nitrogen of **9a_{1&2}**. From 7 to 40 h the reactant signals continued to decrease; intermediate signals from **9a_{1&2}** began to decrease, while signals from **12** increased and those for **14a** were detected. (Fig. 3 and Table A5) After 106 h of reaction the reactant ¹H NMR spectra and those of **9a_{1&2}** were no longer detectable. After 210 h the spectrum of **10a** was no longer detectable. So the sequence of appearance and disappearance of ¹H NMR signals supports the reaction sequence summarized in Fig. 3, steps **7** + **8a** → **9a_{1&2}** → **10a** → **12** + **14a**. Apparently the increased availability of acidic protons and/or more polar solvent facilitated both the formation and decomposition of **9a_{1&2}** which are stable under reaction conditions in chloroform-*d*. (See Section 3.1.1).

3.2. Reactions of α,β unsaturated carbonyl substrates

3.2.1. Methyl vinyl ketone

As shown in Fig. 4, ¹H NMR monitoring of **7** reacting with methyl vinyl ketone(3-butene-2-one) (**8d**) in chloroform-*d* first showed formation of **9d** (detected at 5 min. and characterized at 24 min.) followed by the simultaneous increase of **12** and appearance of **13d₁** (detected at 24 min. and characterized at 50 min.), then **13d₂** (detected at 50 min. and characterized at 105 min.) and finally appearance of **14d** (detected at 4 h and characterized at 198 h).

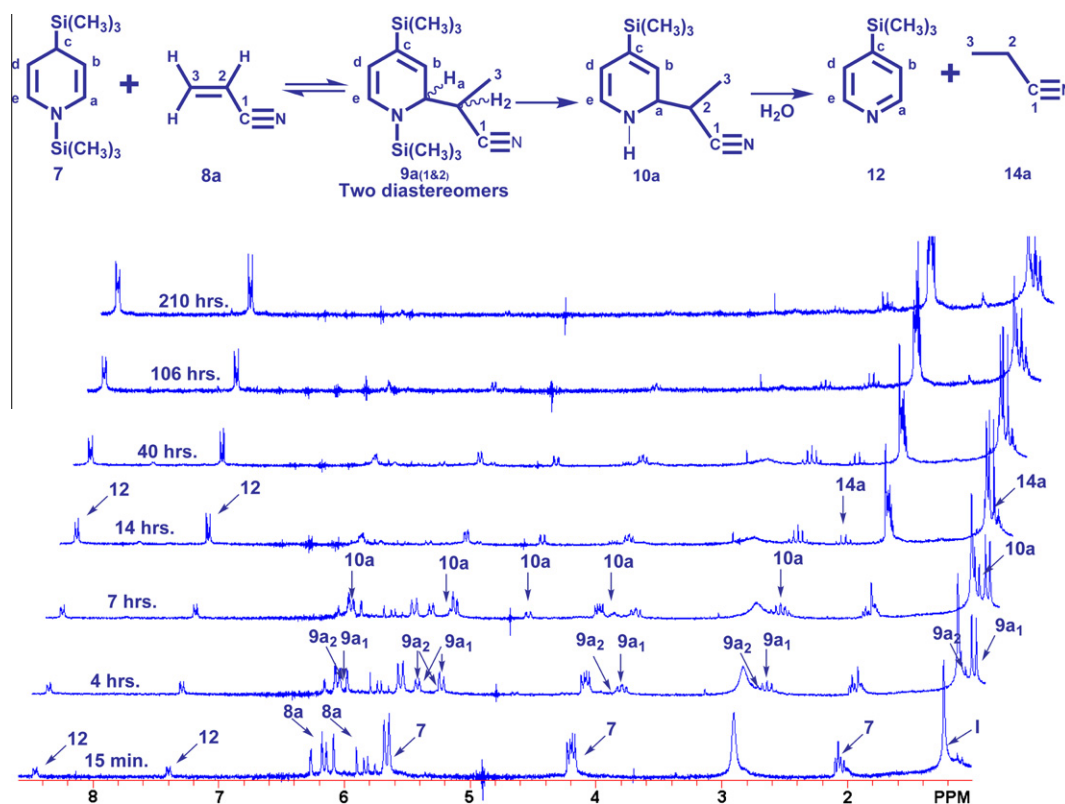


Fig. 3. Reaction of 1,4-di(trimethylsilyl)-1,4-dihydropyridine, **7**, with acrylonitrile, **8a**, in acetone- d_6 /H $_2$ O: starting material **7** and **8d** and irremovable impurities **12** and **14** from **7** are labeled in the first time point. Intermediates and products are labeled at times when they were first characterizable. Chemical shifts: **7**: H(a&e) 5.66 δ , H(b&d) 4.25 δ dd, Hc 2.11 δ t; **8a**: H $_2$ 5.84 δ dd, H $_{3cis}$ 6.12 δ dd, H $_{3trans}$ 6.23 δ dd, I: 1.24 δ s; **water**: 2.90 δ s; **9a $_1$** : Ha 3.90 δ dd, Hb 5.53 δ d, Hd 5.35 δ d, He 6.17 δ d, H $_2$ 2.74 δ dq, H $_3$ 1.11 δ d; **9a $_2$** : Ha 4.08 δ dd, Hb 5.53 δ d, Hd 5.38 δ m, He 6.18 δ d, H $_2$ 2.88 δ m, H $_3$ 1.20 δ d; **10a**: Ha 4.08 δ dd, Hb 5.37 δ d, Hd 4.76 δ d, He 6.17 δ d, H $_2$ 2.73 δ dq, H $_3$ 1.19 δ d; **12**: H(a&e) 8.45 δ dd, H(b&d) 7.40 δ dd; **14a** H $_2$ 2.37 δ q, H $_3$ 1.17 δ t. (See Tables A1–A5 for coupling constants.)

Intermediates **13d**_(1&2) are formed as a mixture of *E*–*Z* isomers with distinct $^1\text{H NMR}$ spectra as indicated (Fig. 4). The *E*–*Z* isomers were formed in a ratio of approximately **13d**₁:**13d**₂ = 4:1 based on the relative integrations of the 1.71 δ and 1.68 δ signals. The formation of **13d**₁ and **13d**₂ from **9d** may occur in one-step because of the possibility of a six-atom cyclic reaction step that concertedly transfers the trimethylsilyl group from the ring nitrogen to the substituent oxygen. (Scheme A1) Alternatively, conversion of **9d** to **13d** + **12** may be a stepwise process with **10d** as an intermediate present at a steady state concentration too low to be observed by $^1\text{H NMR}$. (Scheme A2) Intermediates **13d**_(1&2) progress slowly to **14d** in chloroform-*d* solution. Intermediate **9d** was no longer detectable by $^1\text{H NMR}$ after 4 h of reaction, and intermediate **13d** was still the major product when reaction monitoring was terminated at 198 h. The sequence of appearance of intermediates (**9d**, then **12** and **13d**₁, followed by **13d**₂ and then **14d**) support the reaction sequence **7** + **8d** \rightarrow **9d** \rightarrow **12** + **13d** \rightarrow **14d** illustrated in Fig. 4.

The reaction of **7** with **8d** in acetone- d_6 without added water (Fig. A4 and Tables A5–A7) progressed very similarly but a bit more slowly than the reaction in chloroform-*d*: **9d** signals detected within 40 min, those for **12** and **13d**_(1&2) appeared after 2 h, **14d** signals detected after 10 h, however, the chemical shifts and coupling constants for individual peaks were slightly different (Tables A4–A7, acetone- d_6). As with the reaction in chloroform-*d*, formation of **14d** in acetone- d_6 was sufficiently slow that **13d**_(1&2) were still the major species present after 139 h of reaction. So the reaction path for **8d** with **7** in acetone- d_6 is the same as that in chloroform-*d*. (Fig. 4: **7** + **8d** \rightarrow **9d** \rightarrow **12** + **13d** \rightarrow **14d**).

As with reactions of cyano substrates, addition of water to the reaction of **8d** with **7** in acetone- d_6 led to a significantly faster process compared to their reactions in chloroform-*d* or acetone- d_6 alone (Fig. 4, A4 and A5). After 15 min. of reaction in the presence of water, **9d** was barely detectable from its two major signals at 2.0 and 0.89 δ and within 40 min of mixing, signals for **13d**_(1&2), **12** (increase) and **14d** were detected simultaneously. (Fig. A5 and Tables A5–A7) For the first 48 h of the reaction, the signals for **13d**_(1&2) increased slowly as the signals for **12** and **14d** increased more rapidly and those for **7**, **8d** and H $_2$ O decreased. After 48 h of reaction the signals for **13d**_(1&2) began to decrease in intensity as signals for **12** and **14d** continued to increase. While intermediate spectra were less intense than for reactions in the absence of water, all aspects for the reaction of **8d** with **7** in the presence of added water are consistent with the mechanism observed in chloroform-*d* and acetone- d_6 in the absence of water, **7** + **8d** \rightarrow **9d** \rightarrow **12** + **13d** \rightarrow **14d** (Fig. 4 and Tables A5–A7). The lower intensities of NMR spectra of **9d** and **13d**_(1&2) and the earlier appearance of the product, **14d**, suggest that the rates of decomposition of **9d** and **13d**_(1&2) are more rapid in the presence of water than in its absence (Figs. A4 and A5).

3.2.2. Methyl acrylate

The first detectable intermediate in the reaction of methyl acrylate (methyl propenoate) **8e** with **7** in acetone- d_6 /H $_2$ O (Fig. 5) is **9e**, detected after 1 h of reaction. As with **9a**, two diastereomers of **9e**_(1&2) were characterized. Three hours after mixing, the intensities of the **9e**_(1&2) signals had increased, signals from methyl propenoate, **14e**, were detected and the signals for **12** had begun to

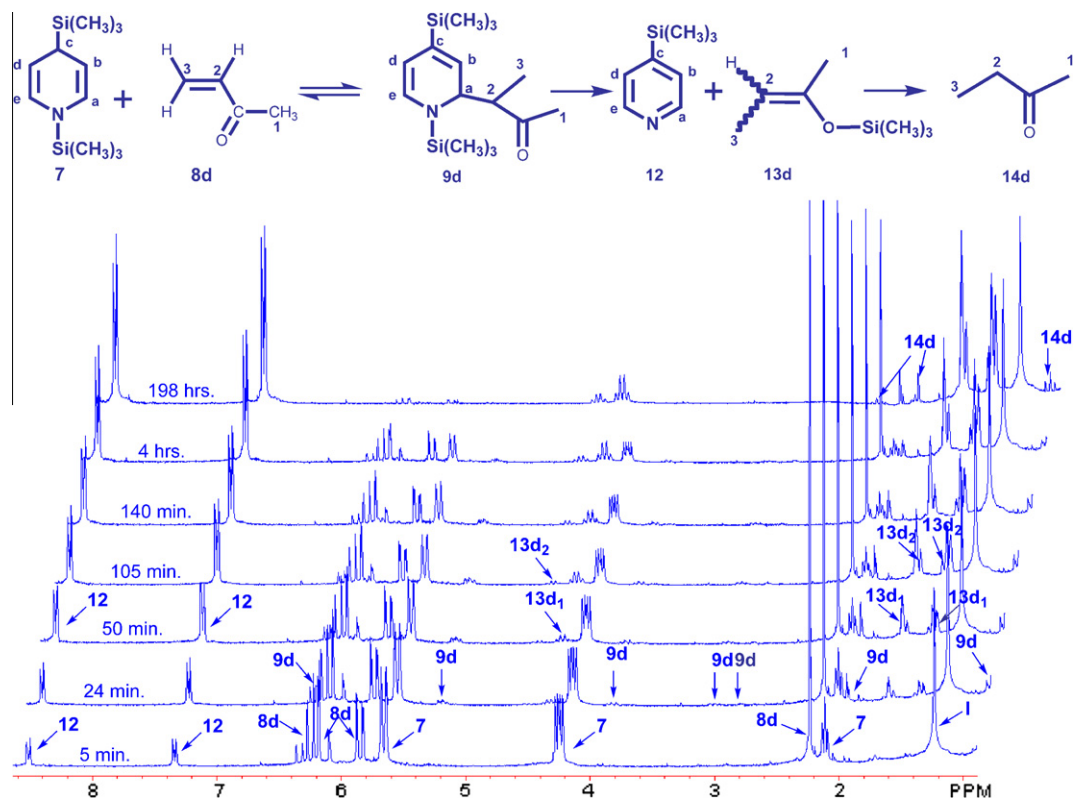


Fig. 4. Reaction of 1,4-ditrimethylsilyl-1,4-dihydropyridine, **7**, with methyl vinyl ketone, **8d**, in chloroform-*d*: starting material **7** and **8d** and irremovable impurities **12** and (**1**) from **7** are labeled in the first time point. Intermediates and products are labeled at times when they were first characterizable. Chemical shifts: **7**, **12** and **1** (See Fig. 2) **8d**: H1 2.24 δ s, H2 5.85 δ dd, H3_{cis} 6.30 δ dd, H3_{trans} 6.14 δ dd; **9d**: Ha 3.12 δ dd, Hb 5.32 δ d, Hc 3.92 δ d, Hd 6.13 δ d, H1 2.05 δ d, H2 2.91 δ dq, H3 0.90 δ d; **13d**₁ H1 1.45 δ dq, H2 4.45 δ qq, H3 1.71 δ dq; **13d**₂ H1 1.47 δ dq, H2 4.63 δ qq, H3 1.68 δ dq; **14d** H1 2.07 δ s, H2 2.45 δ q, H3 0.90 δ t. (See Tables A1–A3 and A5–A7 for coupling constants.)

increase. The intensities of the **9e**_(1&2) signals reached a maximum after 36 h of reaction and then began to decrease. The intensities of the signals from **14e** increased until the signals from **7**, **8e** and **9e**_(1&2) were no longer detectable (172 h of reaction). The reaction of **8e** with **7** showed no ¹HNMR evidence for a **13e** intermediate which would be expected to exhibit signals in the region of 1–2 δ and 4–5 δ as did **13d**. (Fig. 4) So the reaction either follows the mechanistic sequence **9e**_(1&2) \rightarrow **12** + **14e** as illustrated in Fig. 5 or the sequence **9e**_(1&2) \rightarrow **12** + **13e** \rightarrow **14e** where decomposition of **13e** is fast enough that it does not accumulate sufficiently to be detected by ¹HNMR.

4. Discussion

All of our data are consistent with the general Ene mechanism presented in Fig. 6. All reactions of **7** with various acceptors, **8a–e** (Fig. 1) involve an initial Ene reaction (Step A in Fig. 6) forming Ene adducts, **9a–e**. With varying substrate structure or reaction conditions, there are three observable decomposition pathways for **9**, Fig. 6 paths B + E (See Fig. 3), C + F (see Fig. 4), or D (see Fig. 5).

The relative rates of formation of all **9** intermediates seem to increase as solvent polarity is increased with addition of water to the solvent. (see Sections 3.1.2 and 3.2.1) Recent theoretical studies of Retro-Ene reactions of allyl ethers and thioethers, the reverse of Fig. 6, Step A, indicate that they employ an asynchronous concerted mechanism [8]. The transition states of these reactions have some separation of charges. So increases in solvent polarity should have a larger energy lowering effect on the transition states than on the neutral reactants leading to a rate increase.

Rates of decomposition of **9** intermediates under similar conditions seem to follow the order **9d** > **9e** > **9a** (Relative times of disappearance of **9** intermediates in Figs. 3 and 5 and A5, and progress curves of formation of final products in Fig. A6). Regardless of the pathway for decomposition of **9**, at some point the C–C bond between the acceptor substrate and pyridine ring must break. The order of reactivity of the intermediates in this study, increasing with decreasing pK_a value of the product α -atom, suggests that the C–C bond breaks heterolytically leaving extra electron density on the α -atom of the product. Consequently, a greater ability of the acceptor substrate to accommodate the excess electron density should increase the rate of decomposition of **9**. If the atom attached to the pyridine ring in **9** was oxygen, as in many NADH dehydrogenases studied, the rate of decomposition of **9** should be very fast, making the steady-state concentration of **9** very low. Thus, it is not surprising that, even if they do form, analogous Ene intermediates have not been observed in biological systems before now. The data presented here suggest that if such intermediates do form in enzymatic reactions their concentrations should be very low.

The chemical shifts in the ¹HNMR spectra of the ring protons in the first observable intermediates, **9a–e**, in the reactions of **8a–e** with **7**, vary only slightly with changes in substrate structure (Tables A3 and 7A). Our spectra for **9a** are consistent with the ¹HNMR spectrum reported by Sulzbach and Iqbal for **9a** (5.9 δ doublet, 5.7 δ doublet, 5.4 δ doublet, 3.6 δ doublet of doublets, 2.6 δ multiplet) [9]. It is clear that all of our reactions form an initial Ene adduct. However, subsequent reactions of **9a,d,e** vary with changes in substrate structure and reaction conditions. Our ability to observe intermediate **9** indicates that step A is initially faster than any of the modes of decomposition of **9**, otherwise spectra

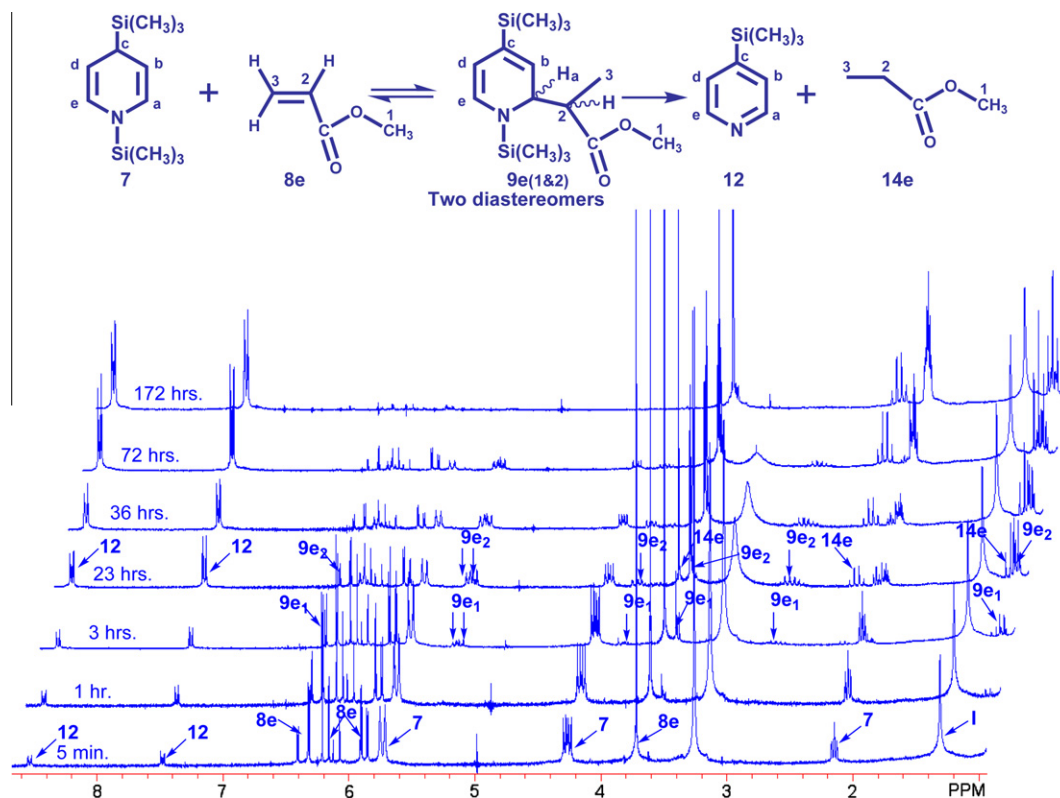


Fig. 5. Reaction of methyl acrylate, **8e**, with 1,4-ditrimethylsilyl-1,4-dihydropyridine, **7**, in acetone- d_6 /water: Starting material **7** and irreremovable impurities **12** and (**1**) from **7** are labeled in the first time point. Intermediates and products are labeled at times when they were first characterizable. Chemical shifts: **7**: H(a&e) 5.66 δ d, H(b&d) 4.25 δ dd, Hc 2.11 δ t; **water**: 3.25 δ s, **8e**: H1 3.65 δ s, H2 5.80 δ dd, H3_{cis} 6.29 δ dd, H3_{trans} 6.07 δ dd; **9e**₁: Ha 3.92 δ dd, Hb 5.38 δ d, Hd 5.33 δ dd, He 6.23 δ d, H1 3.63 δ s, H2 2.84 δ dq, H3 1.04 δ d; **9e**₂: Ha 3.89 δ dd, Hb 5.39 δ d, Hd 5.34 δ dd, He 6.20 δ d, H1 3.64 δ s, H2 2.7–2.9 m, H3 1.02 δ d; **12**: H(a&e) 8.45 δ dd, H(b&d) 7.40 δ dd; **1**: 1.24 δ s; **14e** H1 3.60 δ s, H2 2.31 δ q, H3 1.09 δ t. (See Tables A1, A2, A5 and A6 for coupling constants.)

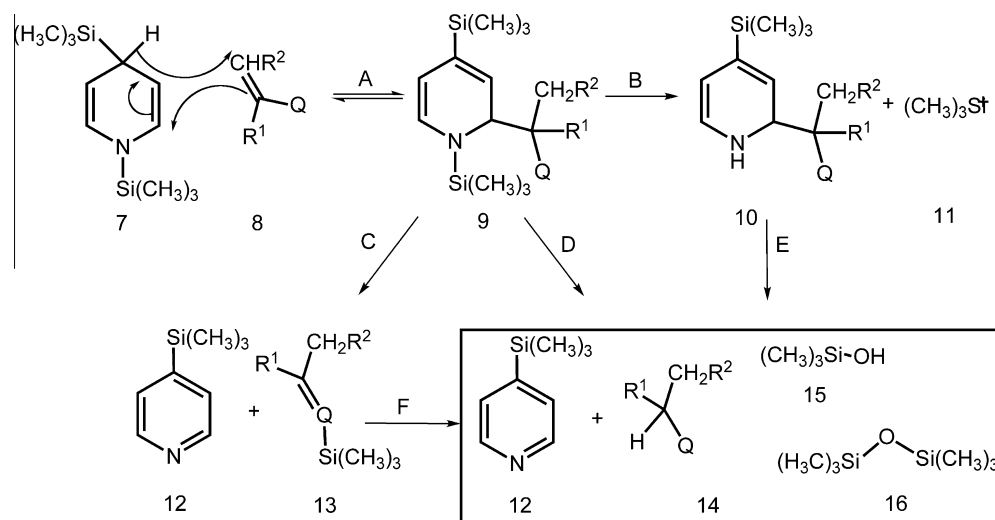
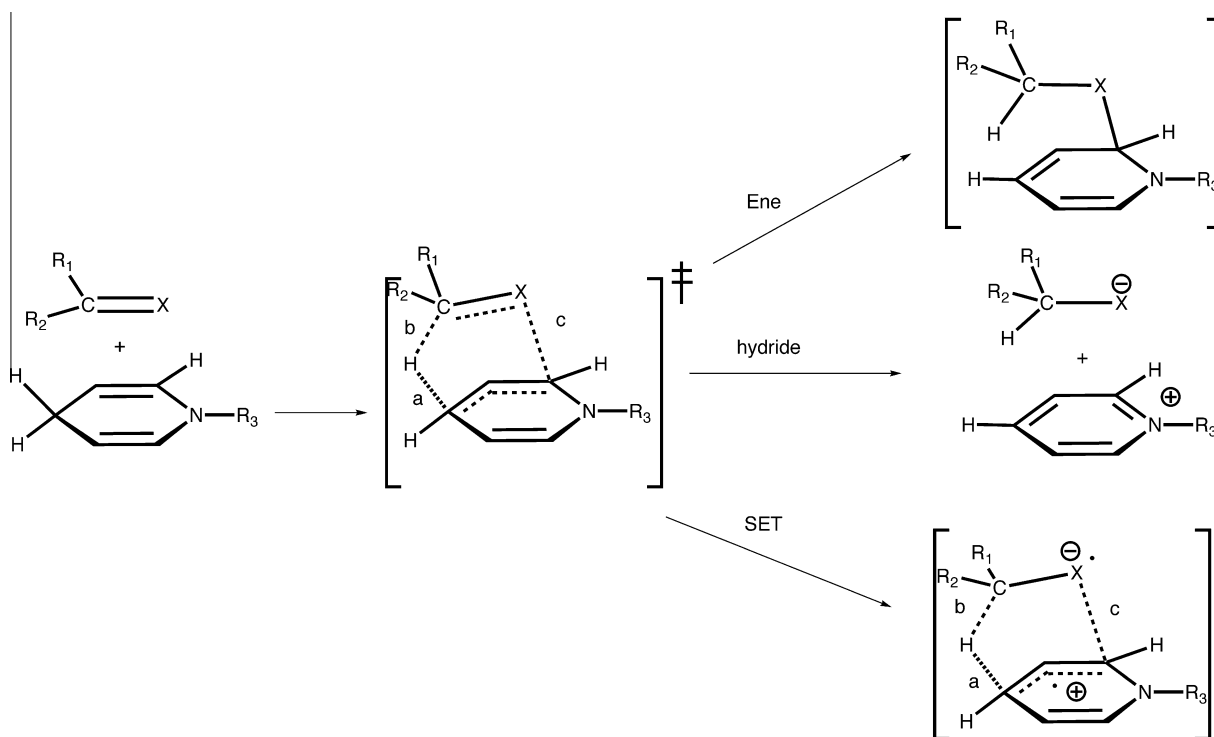


Fig. 6. General mechanistic scheme for the reaction of 1,4-di(trimethylsilyl)-1,4-dihydropyridine, **7**, with acceptor substrates **8a–e**. **8a**: R₁ = R₂ = H, Q = CN; **8b**: R₁ = CH₃, R₂ = H, Q = CN; **8c**: R₁ = H, R₂ = CH₃, Q = CN; **8d**: R₁ = R₂ = H, Q = COCH₃; **8e**: R₁ = R₂ = H, Q = COOCH₃.

of **9** would not have been detectable. So all of our reactions involve a covalent intermediate in the dihydropyridine reduction process.

Previous NADH redox model studies have provided examples singlet electron transfer (SET) and apparently concerted (no detectable intermediate) mechanisms [2,8,10–14]. Our identification of covalent intermediates, **9a,d,e**, completes the spectrum of observed mechanisms with NADH model reactions. Results from

reactions of dihydropyridines and a wide range of model compounds seem to involve one of these mechanisms. We suggest that a general initial Ene-shaped transition state structure could accommodate all three mechanisms for transferring a hydride equivalent. Scheme 1 describes the general shape of a transition state that is consistent with the model reactions, theoretical calculations and biological data.



Scheme 1. Ene-shaped dehydrogenase transition state structure.

The cyclic transition state shape provides a six atom delocalized structure which is aromatic. The aromaticity lowers the transition state energies for these reactions compared with transition states that lack the cyclic structure. We suggest that, depending on the structures of reactants and any catalyst, transition states would vary in the distances labeled a, b and c in Scheme 1. Variations in these distances could result in any of the three observed reaction paths from a common transition framework.

From a theoretical investigation of reactions of dihydropyridines, Inagaki and Hirabayashi [10] concluded that the key orbital interactions in hydrogen transfer reactions between dihydropyridines and acceptor π -bonds are those between the π orbital of the C2–C3 (or C5–C6) bond in the dihydropyridine and the π^* orbital of the acceptor molecule. Their model indicates that as the acceptor π^* orbital energy is lowered there is a more favorable interaction with the dihydropyridine π orbital; such an interaction would favor an Ene mechanism. They further suggested that sufficient lowering of the acceptor π^* orbital energy could lead to a concerted two-electron transfer between the two π systems in a single step. Although they did not consider the effects of changes in the π orbital of the dihydropyridine, it would follow that raising the energy of that orbital should favor the formation of an Ene adduct. Since the two trimethylsilyl groups in **7** are more electron donating to the dihydropyridine ring than the corresponding substituents in NADH, they should raise the energy of the π orbitals in **7** relative to those in NADH favoring the formation of Ene adducts. Our results prove that, under appropriate conditions, the dihydropyridine ring can support the type of Ene reaction chemistry suggested by Hamilton.

Yasui and Ohno have suggested that a solution to the dichotomy of concerted vs. multi-step reaction sequences for these reactions might be to consider a range of reaction paths with varying energies of potential intermediates and transition states [11]. Our proposal provides a structural shape of an initial transition state that meets the variability described conceptually by Inagaki and Hirabayashi and the mechanistic flexibility proposed by Yasui and Ohno [10,11].

From their *ab initio* calculations on the reaction between methyleniminium ion and dihydropyridine, Wu and Houk proposed a transition state model that involved interaction of the π^* orbitals of the C₃–C₄ bond of NAD⁺ and the π orbital of the acceptor molecule [12]. They treated the hydrogen as a hydride ion and described its interactions with the π bonds between C₄–C₃ on NAD⁺ and C–N of the iminium ion. Although they did not mention involvement of the orbital associated with C₂ or C₆ of NAD⁺, the geometry of their lowest energy syn transition state places the reacting atoms in a cyclic orientation similar to that suggested in Scheme 1 with a relatively long distance represented by c. More recent *ab initio* work on the transition state for hydride transfer between dihydropyridine and pyridinium ion also yielded a syn type transition state in which orbital interactions between the two rings were cited as factors that lower the transition state energy [13]. Schiott, Zheng and Bruice did calculations using a continuum solvation model for the hydride transfer from formate ion to NAD⁺ as a model for the reaction catalyzed by formate dehydrogenase. Their calculated ¹⁵N isotope effects agreed with experimental values, however, they reported that the transition states for addition of formate ion to the 2, 4 or 6 position of the NAD⁺ ring had lower energies than that for the hydride transfer reaction [14]. They concluded that the enzyme must orient the substrate to prevent this competing reaction. Addition of formate ion to the 2 or 6 position of the ring is the first step in the Ene mechanism (Eq. (2)).

There have been many studies of both primary and secondary isotope effects on nicotinamide dependent enzymatic reactions [15]. The lack of a secondary deuterium isotope effect for 2-deuterio-NAD⁺ with alcohol dehydrogenase suggests that the 2 position of the NAD ring does not change its bonding significantly in the reaction [16]. In our general Ene-type transition state, the substrate oxygen would have to be interacting with C₆ of the nicotinamide ring as in intermediate **6** of Eq. (2). Thus, for the cyclic transition state to be involved in enzymatic reactions, the oxygen atom of the alcohol substrate must be positioned so that it is able to interact with C₆ of the NAD ring. Recent X-ray crystallographic data on alcohol dehydrogenase ternary complexes provides some

insight [17]. With a series of substrate analogs, all of the structures of ternary complexes of enzyme, nicotinamide and substrate analogs that place the alcohol carbon atom within 4.0 Å of C₄ of the nicotinamide ring also place the substrate analog oxygen over the ring and within 4.0 Å C₆ of the ring.² Very little movement would be required for the alcohol oxygen to be in position to bond or at least have significant orbital interaction with C6 of NAD⁺. Crystal structures of complexes of lactate and malate dehydrogenases [18] also place substrate analog oxygen atoms over the NAD ring. With isocitrate dehydrogenase one structure shows the substrate analog oxygen oriented away from the NADP⁺ ring, while another places the oxygen closer to C6 of the NADP⁺ than is the hydrogen to be transferred to C4 [19]. (See Appendix A2 for additional crystal data.) It is clear that the crystal structures of ternary complexes are just pictures of relatively stable orientations of substrates on the enzyme surfaces and do not necessarily represent transition state structures, however the majority of the available data does not rule out the possibility of our proposed initial, general, cyclic Ene-shaped transition state structure in these nicotinamide dehydrogenases.

Recently there has been much work using molecular dynamics in conjunction with semi-empirical and *ab initio* approaches to explore pathways of enzymatic catalysis and determine transition state structures on enzyme surfaces [20]. These studies use experimentally determined enzyme complex structures as starting points for their calculations of reaction pathways and transition state structures. Most studies have focused on the distances between the hydrogen nucleus being transferred and its adjacent carbon atoms as well as the C–H–C bond angles in the transition states. Consequently, little information has been reported on the distance between the substrate oxygen and either C₂ or C₆ of the NAD ring. However, the two-dimensional diagrams of transition states reported appear to be consistent with cyclic Ene-shaped transition states (Scheme 1) in which the relative distances for the interactions at a, b and c vary.

Finally, Bull et al. reported that Finasteride, an α,β -unsaturated amide, which is a mechanism based slow binding inhibitor of steroid 5 α -reductase, forms an adduct with NADH as a consequence of its inhibition of the enzymatic reaction [21]. They isolated the adduct and proposed that it consists of the inhibitor molecule covalently bonded from its α -carbon to C4 of NADH. They supported their structural characterization with mass spectral data showing the presence of the masses of both NADH and Finasteride in the adduct, but their assignment of the position of attachment is based on the similarity of its λ_{\max} , 326 nm, to that of the C4 cyanide adduct of NADH, reported as “in the region of 340 m μ ” [22]. However, with the correspondence of the Finasteride adduct λ_{\max} to that of **9a**, 326 nm (see Section 2.7), their data seem equally consistent with attachment of the Finasteride α -carbon to the 6-position of the NADH. Thus, the isolated adduct could be a dead end Ene adduct formed in an Ene reaction of NADH and Finasteride. Our data suggest that the rate of decomposition of the Ene-adducts, **9a,d,e**, vary inversely with the pK_a of the product (see Section 4); it is not surprising that an Ene adduct between NAD and Finasteride would form and decompose very slowly. Binding to the enzyme might also stabilize the adduct producing an effective tight binding inhibitor of the enzyme.

5. Conclusions

Although our 1,4-ditrimethylsilyl-1,4-dihydropyridine model differs significantly from NADH, it contains 1,4-dihydropyridine ring that reduces organic substrates. Our results produce the first

documentation of a covalent intermediate in a 1,4-dihydropyridine redox reaction and provide an example of the Ene mechanism for nicotinamide reactions first proposed by Hamilton. We do not suspect that all nicotinamide redox reactions involve an Ene intermediate, but we do suggest that this demonstration of the ability of dihydropyridines to support Ene reactions provides a more general model for a versatile initial Ene-shaped transition state structure (Scheme 1) which could account for the variety of observed mechanistic paths in nicotinamide model reactions and is consistent with the vast majority of the available experimental data and theoretical studies on enzymatic systems. The aromatic character of this cyclic transition state structure also provides a theoretically sound explanation for the high rates of the chemical steps of many nicotinamide dehydrogenases. Our proposal changes the concept of the shape of the dehydrogenase transition state and provides a new model for design of potential tight binding inhibitors for NAD dehydrogenases.

Acknowledgment

We thank professor Carl Salter, Moravian College Chemistry Department for many important suggestions in the preparation of this manuscript.

Appendix A. Supplementary material

Supplementary data associated with this article can be found, in the online version, at [doi:10.1016/j.bioorg.2011.10.002](https://doi.org/10.1016/j.bioorg.2011.10.002).

References

- [1] F.H. Westheimer, H.F. Fisher, E.E. Conn, B. Vennessland, Enzymatic transfer of hydrogen to DPN, *J. Am. Chem. Soc.* 73 (1951) 2403.
- [2] (a) F.H. Westheimer, Mechanism of action of the pyridine nucleotides, in: D. Dolphin, O. Avramovic, R. Poulson (Eds.), *Pyridine Nucleotide Coenzymes: Chemical, Biochemical, and Medical Aspects*, Part A, John Wiley & Sons, New York, 1987, pp. 253–322; (b) N.J. Oppenheimer, A.L. Handlon, third ed., in: D. Sigman (Ed.), *Mechanism of NAD-dependent enzymes*, The Enzymes, vol. 20, Academic Press, Inc., San Diego, CA, 1992, pp. 453–505; (c) S. Yasui, M. Okamura, M. Fujii, Multistep mechanism for “hydride” transfers in the redox reactions induced by NAD(P)H- and NAD(P)⁺-models, *Rev. Het. Chem.* 20 (1999) 145–165.
- [3] G.A. Hamilton, Proton in biological redox reactions, *Prog. Bioorg. Chem.* 1 (1971) 83–157.
- [4] (a) L.J. Rodriguez, A.B. Vidal, R.E. Izquierdo, J.R. Fermin, R. Anez, Activation energy calculation for retro-ene elimination reaction of propylene from diallyl ether, *Theochem* 769 (2006) 211–216; (b) A. Viola, J.J. Collins, N. Filipp, Intramolecular pericyclic reaction of acetylenes. Part 9. Intramolecular pericyclic reactions of acetylene compounds, *Tetrahedron* 37 (1981) 3765–3811. and references therein; (c) T. Ibuki, Y. Takezaki, Unimolecular decomposition of chemically activated methyl allyl ether, *Int. J. Chem. Kinect.* 9 (1977) 201–213; (d) P. Vitins, K.W. Egger, Thermochemical kinetics of retro-ene reactions of molecules with the general structure (allyl)XYH in the gas phase. IX. Unimolecular thermal decomposition of diallyl ether, *J. Chem. Soc. Perkin II* 11 (1974) 1292–1293; (e) K. W. Egger, P. Vitins, Thermochemical kinetics of retro ene reactions of molecules with the general structure (allyl)XYH in the gas phase. IX. Thermal unimolecular decomposition of ethyl allyl ether in the gas phase, *Int. J. Chem. Kinect.* 6 (1974) 429–435.
- [5] K. Alder, F. Pascher, A. Schmitz, Substituting additions. I. Addition of maleic anhydride and azodicarboxylic esters to singly unsaturated hydrocarbons. Substitution processes in the allyl position, *Chem. Ber.* 76 (1943) 27–53.
- [6] L.F. Fieser, M. Fieser, *Reagents for Organic Synthesis*, vol. 1, John Wiley & Sons, Inc., 1967, pp. 1140.
- [7] R.A. Sulzbach, Synthesis and properties of 1,4-bis(trimethylsilyl)-1,4-dihydropyridine, *J. Organomet. Chem.* 24 (1970) 307–314.
- [8] (a) M. Izadyar, A.H. Jahangir, M.R. Gholami, DFT calculations on retro-ene reactions part I: allyl *n*-butyl sulfide pyrolysis in the gas phase, *J. Chem. Res.* 9 (2004) 585–588; (b) M. Izadyar, M.R. Gholami, M. Haghgu, DFT calculations on retro-ene reactions, part II: allyl *n*-propyl sulfide pyrolysis in the gas phase, *Theochem* 686 (2004) 37–42.
- [9] R.A. Sulzbach, A.F.M. Iqbal, Addition of acrylonitrile to derivatives on 1,4-dihydropyridine, *Angew. Chem. Int. Ed. Eng.* 10 (1971) 733.

² Distances determined from coordinates in files 1AXE.PDB, 1QV6.PDB, 1QV7.PDB and 1MGO.PDB.

- [10] S. Inagaki, Y. Hirabayashi, Mechanism of NAD(P)H reduction reactions, *Bull. Chem. Soc. Jpn.* 50 (1977) 3360–3364.
- [11] S. Yasui, A. Ohno, Model studies with nicotinamide derivatives, *Bioorg. Chem.* 14 (1986) 70–96.
- [12] T.-D. Wu, K.N. Houk, Theoretical transition structures for hydride transfer to methyleneiminium ion from methylamine and dihydropyridine. On the nonlinearity of hydride transfers, *J. Am. Chem. Soc.* 109 (1987) 2226–2227.
- [13] T.-D. Wu, D.K.W. Lai, K.N. Houk, Transition structures of hydride transfer reactions of protonated pyridinium ion with 1,4-dihydropyridine and protonated nicotinamide with 1,4-dihyronicotinamide, *J. Am. Chem. Soc.* 117 (1995) 4100–4108.
- [14] B. Schiott, Y.-J. Zheng, T.C. Bruice, Theoretical investigation of the hydride transfer from formate to NAD⁺ and the implications for the catalytic mechanism of formate dehydrogenase, *J. Am. Chem. Soc.* 120 (1998) 7192–7200.
- [15] P.F. Cook, B.L. Bertagnolli, Kinetics of pyridine nucleotide utilizing enzymes, in: D. Dolphin, O. Avramovic, R. Poulson (Eds.), *Pyridine Nucleotide Coenzymes: Chemical, Biochemical, and Medical Aspects, Part A*, John Wiley & Sons, New York, 1987, pp. 405–447.
- [16] (a) P.F. Cook, N.J. Oppenheimer, W.W. Cleland, Secondary deuterium and nitrogen-15 isotope effects in enzyme-catalyzed reactions. Chemical mechanism of liver alcohol dehydrogenase, *Biochemistry* 20 (1981) 1817–1825;
(b) J.W. Burgner II, N. J Oppenheimer, W.J. Ray, Remote nitrogen-15 isotope effects on addition of cyanide to NAD, *Biochemistry* 26 (1987) 91–96;
(c) N. Rotberg, W.W. Cleland, Secondary nitrogen-15 isotope effects on the reactions catalyzed by alcohol dehydrogenases, *Biochemistry* 30 (1991) 4068–4071.
- [17] (a) S. Ramaswamy, H. Eklund, B.V. Plapp, Structure of horse liver alcohol dehydrogenase complexed with NAD⁺ and substituted benzyl alcohols, *Biochemistry* 33 (1994) 5230–5237;
(b) L.A. LeBrun, D.-H. Park, D.-H.S. Ramaswamy, B.V. Plapp, Participation of histidine-51 in catalysis by horse liver alcohol dehydrogenase, *Biochemistry* 43 (2004) 3014–3026;
(c) J.K. Rubach, B.V. Plapp, Mobility of fluorobenzyl alcohols bound to liver alcohol dehydrogenases as determined by NMR and X-ray crystallographic, *Biochemistry* 41 (2002) 15770–15779.
- [18] (a) D.B. Wigley, S.J. Gamblin, J.P. Turkenburg, E.J. Dodson, Piontek, H. Muirhead, J.J. Holbrook, Structure of a ternary complex of an allosteric lactate dehydrogenase from *Bacillus stearothermophilus* at 2.5 Å resolution, *J. Mol. Biol.* 223 (1992) 317–335;
(b) M.D. Hall, D.G. Levitt, L.J. Banaszak, Crystal structure of *Escherichia coli* malate dehydrogenase. A complex of the apoenzyme and citrate at 1.87 Å resolution, *J. Mol. Biol.* 226 (1992) 867–882;
(c) A.D. Chapman, A. Cortes, T.R. Dafforn, A.R. Clarke, R.L. Brady, Structural basis of substrate specificity in malate dehydrogenases: crystal structure of a ternary complex of porcine cytoplasmic malate dehydrogenase, alpha-ketomalate and tetrahydroNAD, *J. Mol. Biol.* 285 (1999) 703–712.
- [19] (a) J.M. Bolduc, D.H. Dyer, W.G. Scott, P. Singer, R.M. Sweet, D.E. Koshland Jr., B.L. Stoddard, Mutagenesis and Laue structures of enzyme intermediates: isocitrate dehydrogenase, *Science* 268 (1995) 1312–1318;
(b) B.L. Stoddard, A. Dean, D.E. Koshland Jr., Structure of isocitrate dehydrogenase with isocitrate, nicotinamide adenine dinucleotide phosphate, and calcium at 2.5-Å resolution: a pseudo-Michaelis ternary complex, *Biochemistry* 32 (1993) 9310–9316.
- [20] (a) T.C. Bruice, A view at the millennium: the efficiency of enzymatic catalysis, *Acc. Chem. Res.* 35 (2002) 139–148;
(b) S. Hammes-Schiffer, S. Billeter, Hybrid approach for the dynamical simulation of proton and hydride transfer in solution and proteins, *Int. Rev. Phys. Chem.* 20 (2001) 591–616;
(c) J. Villa, A. Warshel, Energetics and dynamics of enzymatic reactions, *J. Phys. Chem. B* 105 (2001) 7887–7907.
- [21] H.G. Bull, M. Barcia-Calvo, S. Andersson, W.F. Baginsky, H.K. Chan, D.E. Ellsworth, R.R. Miller, R.A. Sterns, R.K. Bakshi, G.H. Rasmusson, R.L. Tolman, R.W. Myers, J.W. Kozarich, G.S. Harris, Mechanism-based inhibition of human steroid 5α-reductase by Finasteride: enzyme-catalyzed formation of NADP-dihydrofinasteride, a potent bisubstrate analog inhibitor, *J. Am. Chem. Soc.* 118 (1996) 2359–2365.
- [22] S.P. Colowick, N.O. Kaplan, M.M. Ciotti, The reaction of pyridine nucleotide with cyanide and its analytical use, *J. Biol. Chem.* 191 (1951) 447–459.